APPENDIX H

BEG MODELING REPORT

INTENTIONALLY LEFT BLANK

Reservoir modeling and simulation for estimating migration extents of injectate-CO_2 in support of West Ranch oilfield NEPA/EIS

Gulf Coast Carbon Center, Bureau of Economic Geology, Jackson School of Geosciences, The University of Texas at Austin

May 4, 2012

Summary

It is anticipated that anthropogenic carbon dioxide (CO2-A) will be injected into the deep (5,000-6,000 ft below sea level) subsurface for enhanced oil recovery (EOR) at the West Ranch oilfield beginning in early 2015. The purpose of this report is to present reservoir modeling and simulation results generated to support National Environmental Policy Act, Environmental Impact Statement (NEPA/EIS) requirements for the NRG Energy Company's Clean Coal Power Initiative project being funded, in part, by the U.S. Department of Energy, National Energy Technology Laboratory (NETL). The timeframe for the modeling and simulation, injection from 2014 through 2019 with observation extended through 2049, contributes to the conservative nature of the estimate of extent of CO2-A migration. Results show that the extent of the injectate-CO2-A, and associated zones of increased pressure, will remain within the surface footprint of areas leased and operated by Texas Coastal Ventures (TCV, NRG and their oilfield partner Hilcorp Energy) during and beyond the period of concern.

Introduction

Numerous studies have been conducted in the past to characterize subsurface geology below the West Ranch oilfield (e.g. Galloway and Cheng, 1985, ICF Resources and BEG, 1989). Results from these studies, and geologic structural control from geophysical log interpretation using the Petra© project constructed by Hilcorp and BEG, form the basis for the modeling described here. TCV is considering EOR operations in three different reservoir sands in the West Ranch oilfield. From deepest to shallowest these are the 98-A, 41-A, and Greta sand intervals, which are present between approximately 5,000 and 6,000 ft below sea level. Dr. Seyyed Hosseini, Research Associate with the Gulf Coast Carbon Center at the Bureau of Economic Geology, Jackson School of Geosciences, The University of Texas at Austin conducted the modeling and simulation work described herein for the 41-A sand interval as a case example. We consider this example to represent a worse-case scenario of migration of CO2 associated with enhanced oil recovery at the West Ranch oilfield.

Approach

Dr. Hosseini began the reservoir simulation modeling using structure contour data (elevation of top surface) for the 41-A sand constructed in and exported from Petra by Dr. Khandakar Zahid. A uniform thickness of 80 ft was used to generate a parallel bottom surface of this reservoir sand. These surfaces were transferred from Petra to Petrel© modeling software to begin generating the static geologic model for 41-A (fig. 1).

Hosseini then used contract report and published information on the distribution and properties of 41-A sands at West Ranch (figs. 2, 3) to generate a 16-layer reservoir model that represents the geologic setting as realistically as possible. Figure 2 shows the depositional/coastal zone units, or geologic facies, represented in the 41-A reservoir sands along with permeability ranges for each. The facies shown in figure 2 are (1) barrier core, which represents the high permeability sands in the core of a barrier island, (2) moderate permeability tidal channel, and (3) lower permeability tidal delta. Two other facies included in the static geologic model are lagoonal mud and non-sand. In preparing the static

geologic model Hosseini constructed a grid-based distribution of the facies that resembles the Galloway and Cheng (1985) image in figure 2. The model includes both horizontal and vertical heterogeneity as can be seen by the different distributions of facies for model layers 1, 6, and 15 in figures 3a, b, and c.

Based on the formation top information (structure contour map) for the 41-A sand, top surface of the 41-A sand was generated. Bottom surface of the 41-A assumed to be 80 ft below and parallel to the top surface. Surfaces were transferred from Petra to Petrel and static models were generated in Petrel. After generating appropriate structural model (fig. 1), using information published by Galloway and Cheng (1985) (fig.2), appropriate facies model (fig. 3) and corresponding permeability (fig. 4) and porosity (fig. 5) maps were generated. Vertical heterogeneity in the models is considered. Figure 4 shows the permeability distribution in layers 1, 6 and 15.

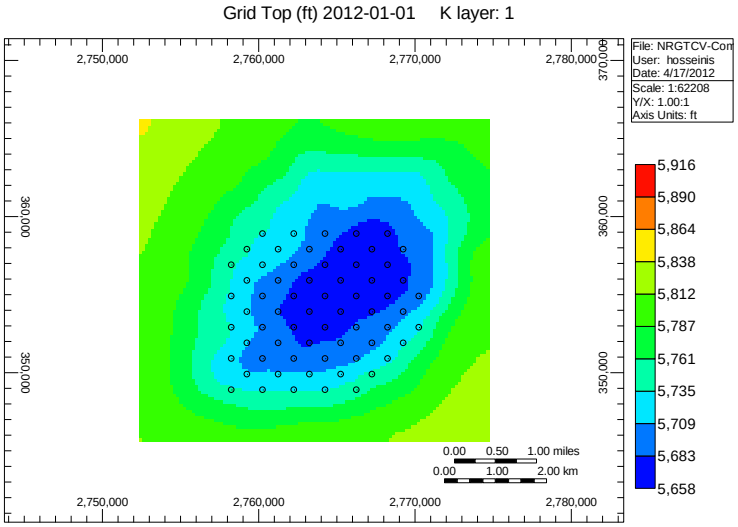

Figure 1. Structure contour map of the top of 41-A sand showing well distribution (open circles) used in reservoir simulations.

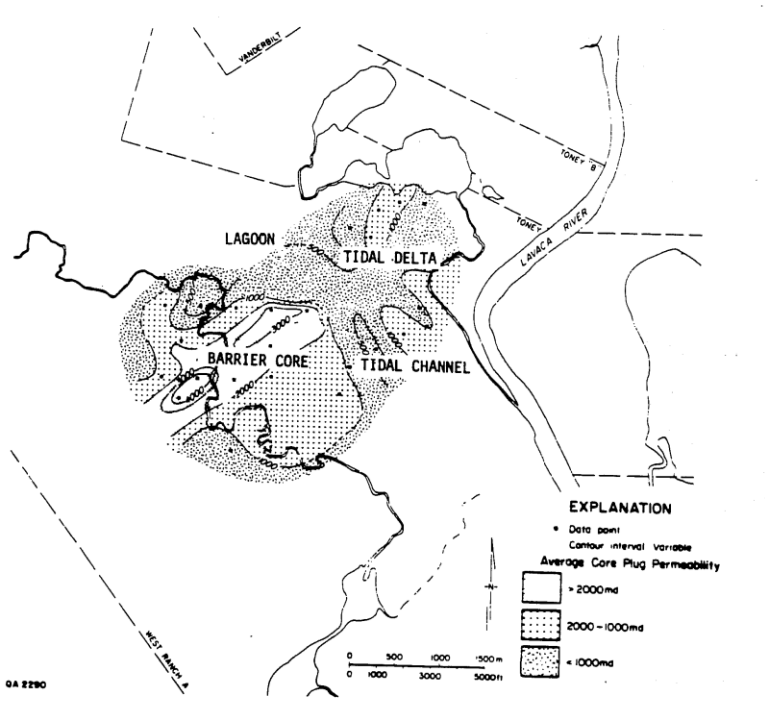

Figure 2. Map of facies and permeability range in the 41-A reservoir. Source: Galloway and Cheng (1985).

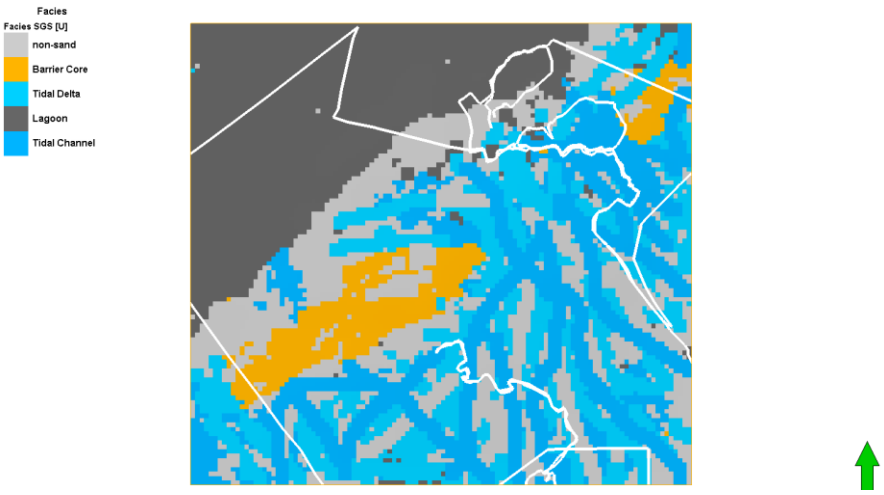

Figure 3a. Facies model for layer 1 of the static model. White lines show TCV lease areas.

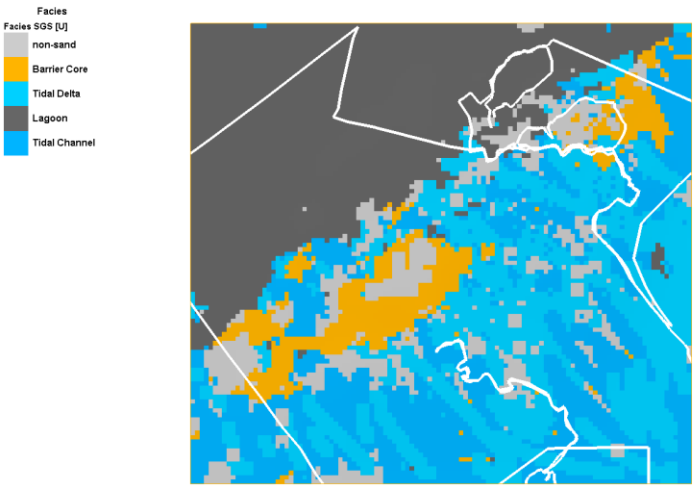

Figure 3b. Facies model for layer 6 of the static model. White lines show TCV lease areas.

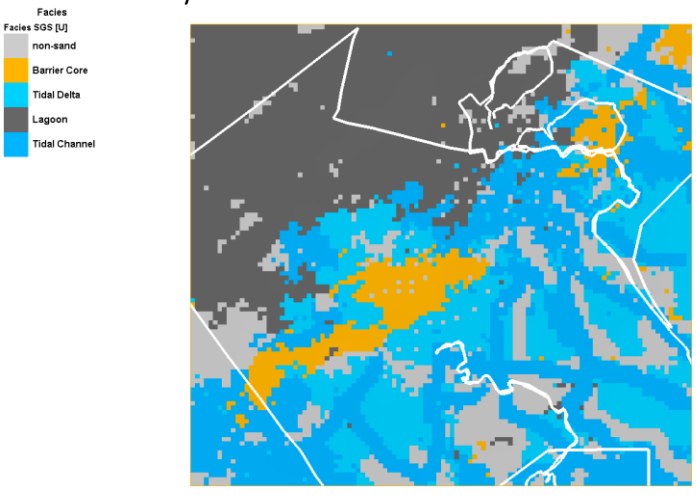

Figure 3c. Facies model for layer 15 of the static model. White lines show TCV lease areas.

The static model layers were then populated with values for permeability based on the ranges shown in for each facies in figure 2, plus a value of less than 10 millidarcies (md) for the lagoon and non-sand facies. Figures 4a, b, and c show variations in permeability corresponding to the facies distributions for model layers 1, 6, and 15. An image of the static porosity component for layer 1 in the reservoir model is shown in figure 5.

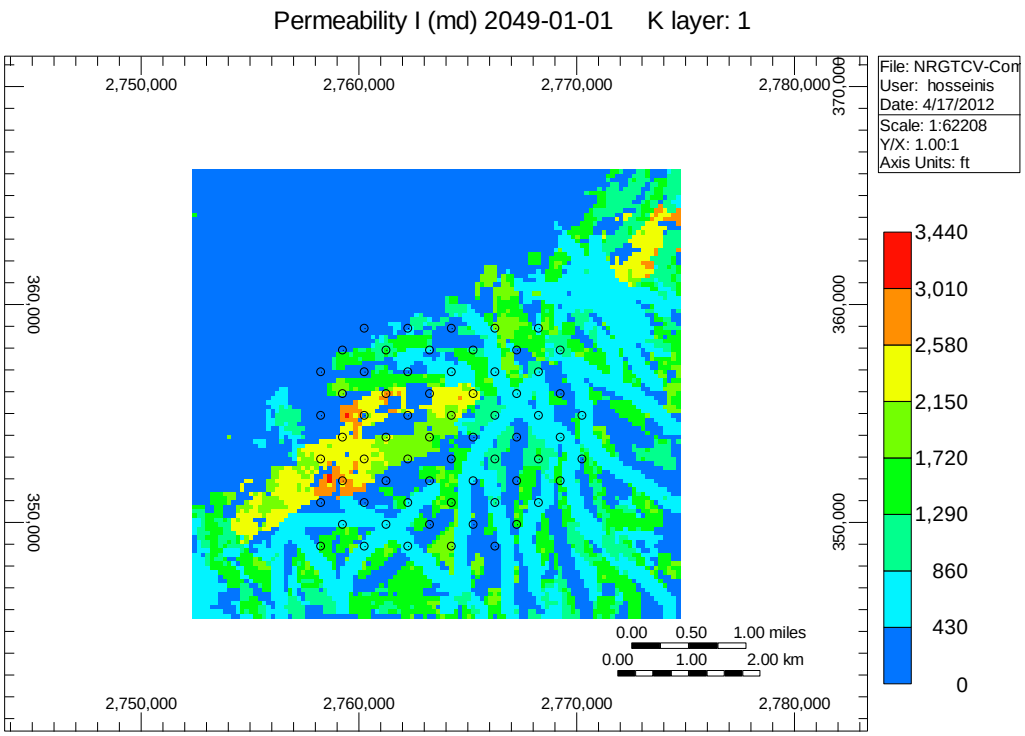

Figure 4a. Permeability model in layer 1 generated based on the facies model, and well distribution (open circles) used in reservoir simulations.

.

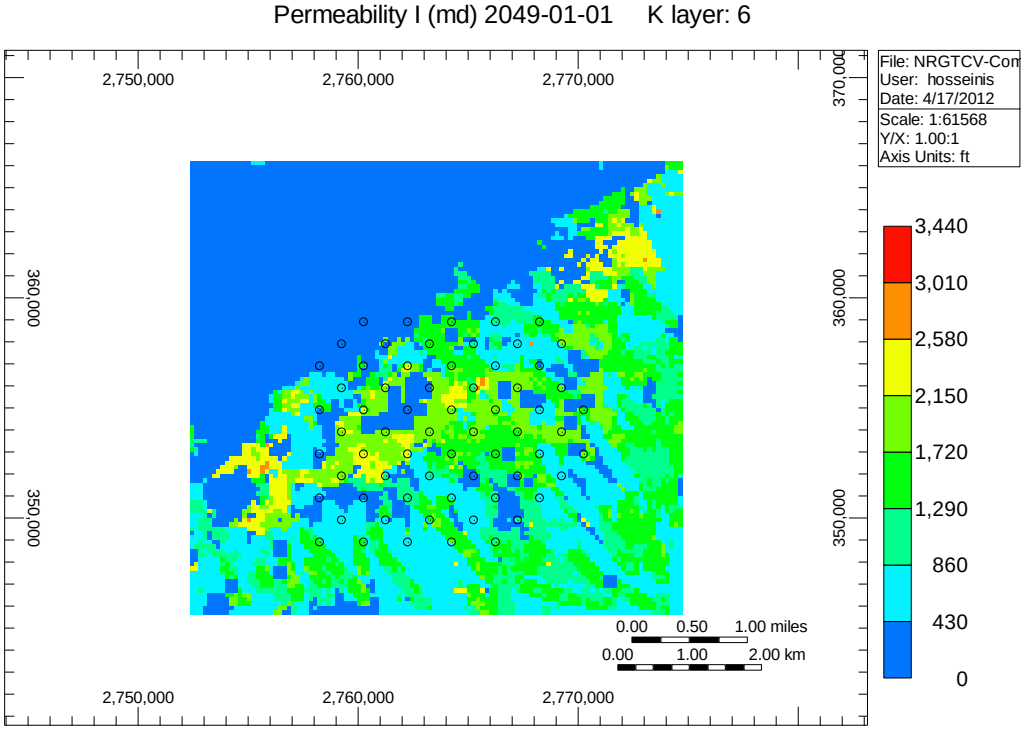

Figure 4b. Permeability model in layer 6 generated based on the facies model, and well distribution (open circles) used in reservoir simulations.

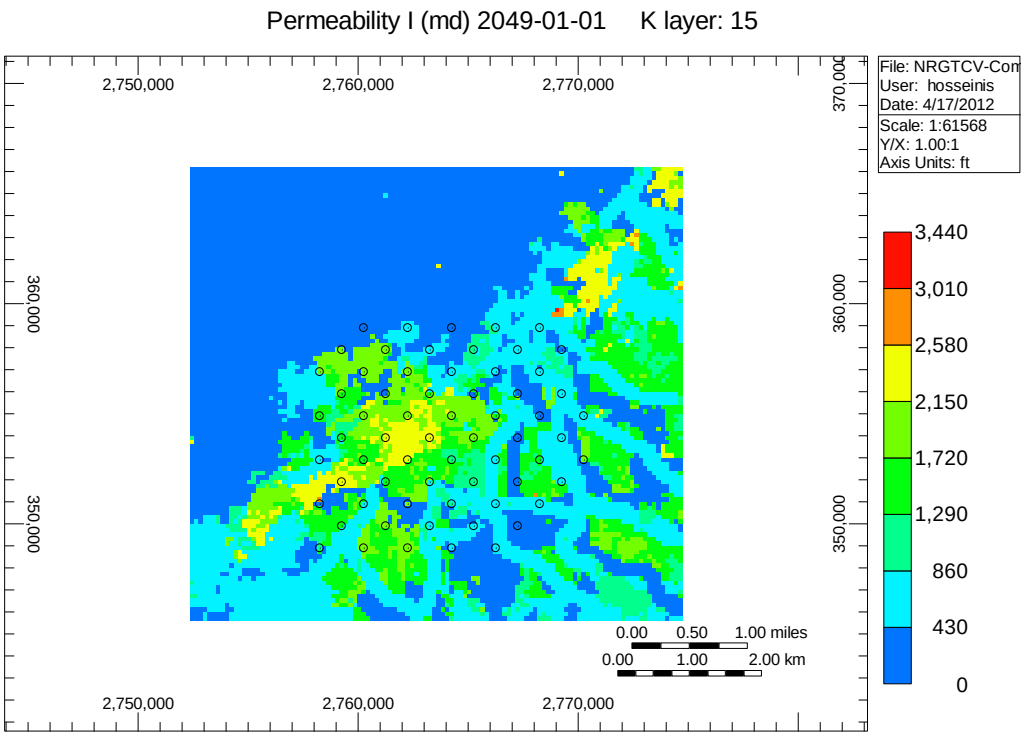

Figure 4c. Permeability model in layer 15 generated based on the facies model, and well distribution (open circles) used in reservoir simulations..

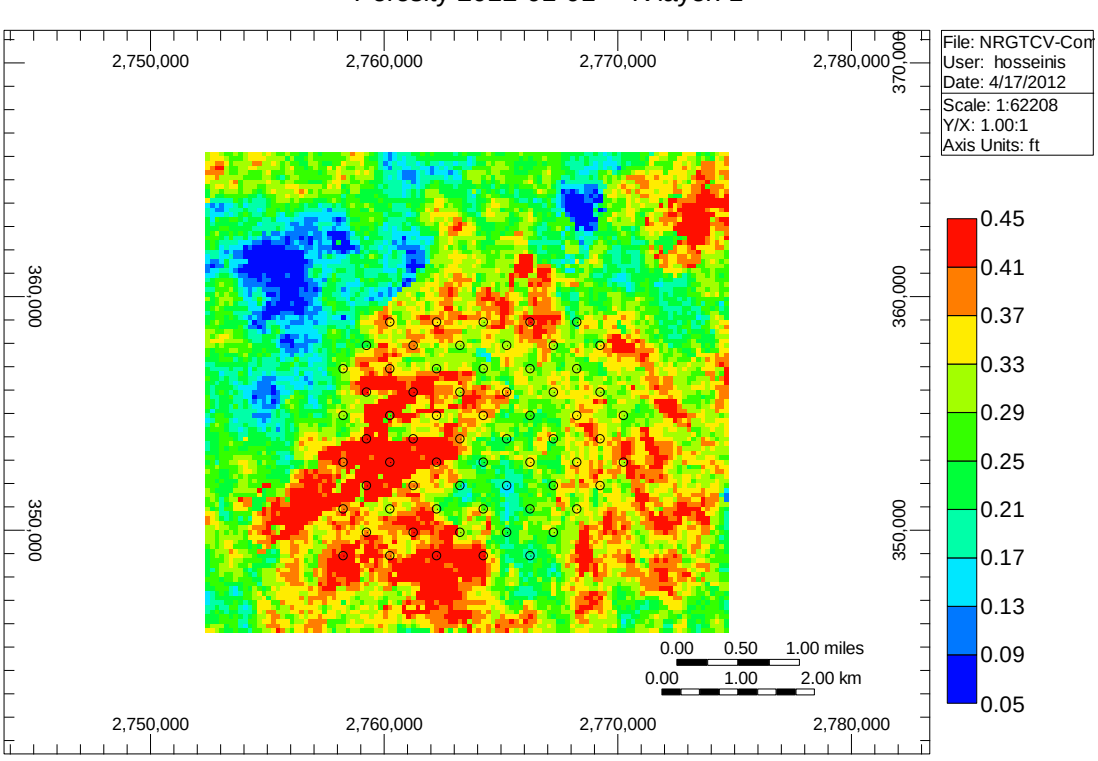

Fig 5. Porosity model for layer 1, and well distribution (open circles) used in reservoir simulations..

After completion, the static model of geologic framework and reservoir fluid properties was transferred to the Computer Modeling Group Ltd. (CMG) GEM© (Generalized Equation-of-State Model) software for dynamic fluid flow modeling. GEM is a compositional reservoir simulator that was used to calculate the extents of injectate CO2 and associated zones of increased pressure. Table 1 gives a summary of important model properties used in the GEM simulations.

Table 1. Properties used for reservoir simulation.

Injection start date	1/1/2014
Injection end date	1/1/2019
Extended simulation date	1/1/2049
Residual oil saturation	0.27
Average porosity	0.30
Average permeability, md	631
Maximum injection rate ,MMscf/day	2.5
Maximum production rate, bbl/day	3000
grids	112×103×16
Grid size, ft	200×200×5
Current reservoir pressure, psi	2400
Kz multiplier	0.1

Figure 6 shows the same wells as in figure 1 superimposed with oil saturation, with the transition from blue to green outlining the oil water contact. There are 36 injection and 29 production wells arranged in five spot patterns. Injection wells were constrained to maximum bottom hole pressure of 3,500 pounds per square inch (psi) and producers were constrained at minimum bottom hole pressure of 2,000 psi. The total injection rate used was about 1.7 million metric tonnes of CO_2 per year. The model was populated with dynamic reservoir data (relative permeability, fluid compositions, minimum miscibility pressure, etc) obtained from reports provided by Hilcorp.

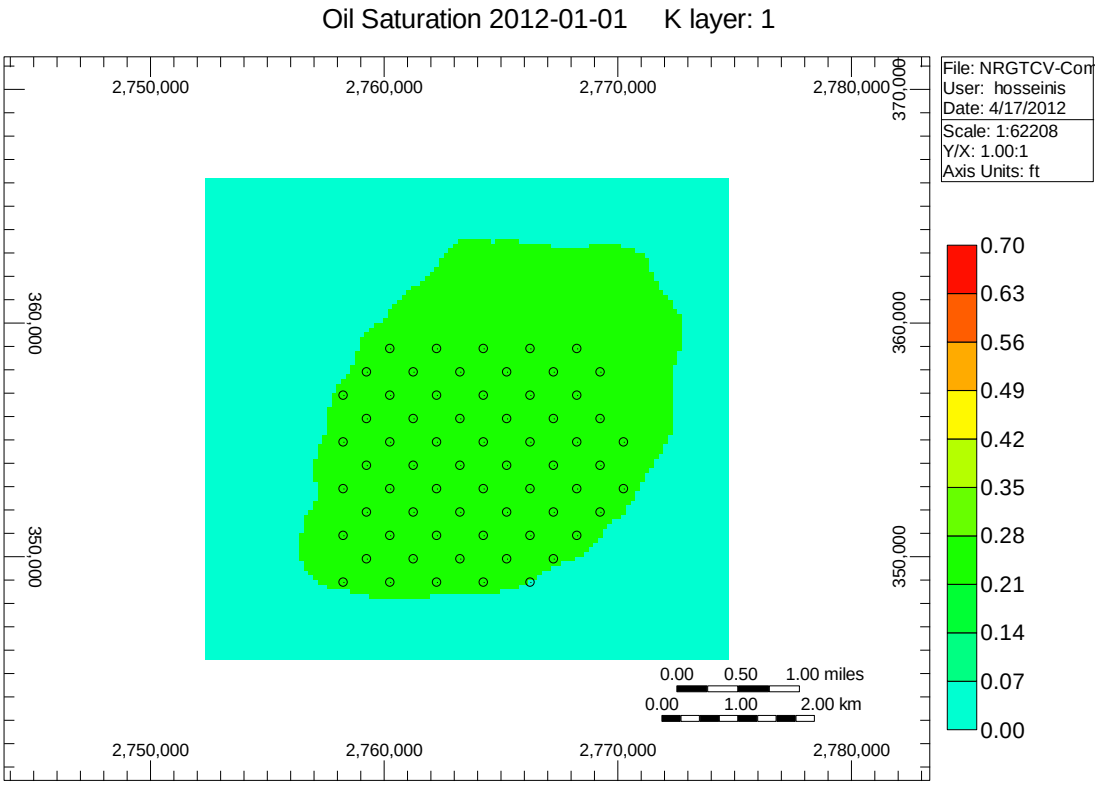

Fig 6. Initial oil saturation showing five-spot well distribution (open circles) used in reservoir simulations.

Results

CO_2 injection was modeled to continue for five years and then all the wells were shut in. The extent of CO2 gas and reservoir pressure after five years is shown for layers 1, 6 and 15 in figures 7 and 8 respectively. Layer 1 is at the top and layer 16 is at the base of the 80-ft thick 41-A reservoir sand. The extent of CO2 is depicted as gas saturation, which represents the pore volume fraction of gas (CO_2). Pressure values are in psi. After all the wells were shut in, an extended simulation was carried out until 2049 to further observe the CO2 migration and pressure response. Extent of the CO2 gas and reservoir pressure after 35 years are shown for layers 1, 6 and 15 in figures 9 and 10, respectively. Due to buoyancy effects most of the gas saturation accumulates in upper layers of the reservoir sand.

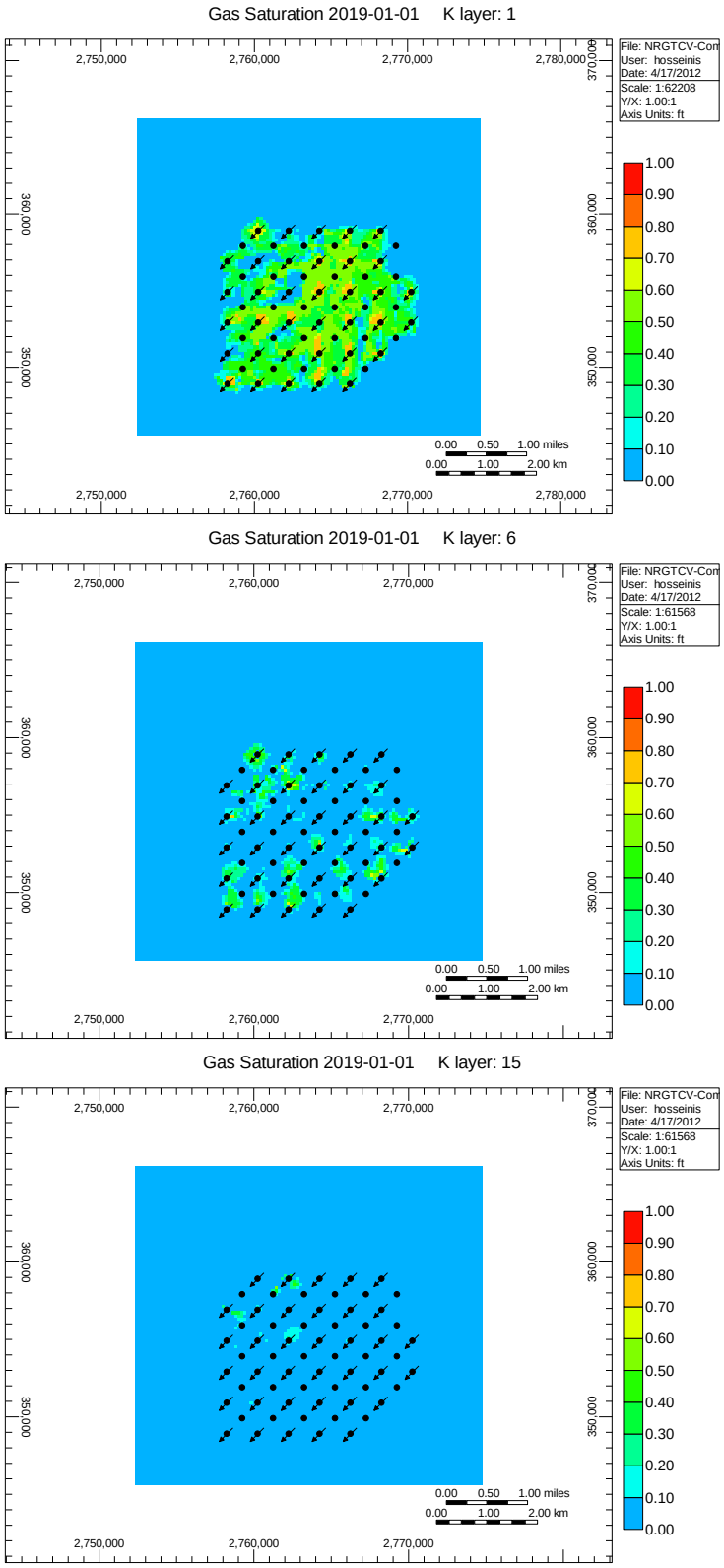

Figure 7. CO_2 extents at 1/1/2019 in layers 1 (top), 6 and 15(bottom)after 5 years of injection.

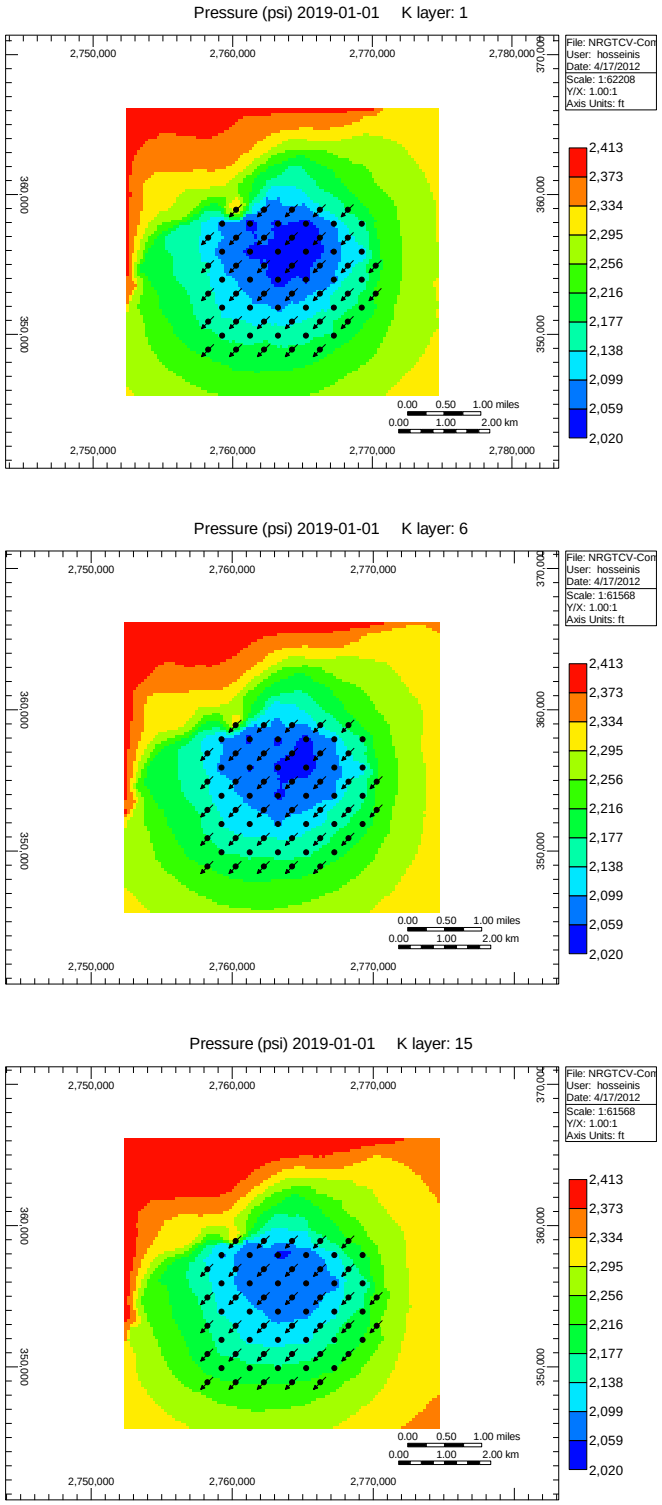

Figure 8. Pressure distribution at 1/1/2019 in layers 1 (top), 6 and 15 (bottom) after 5 years of injection

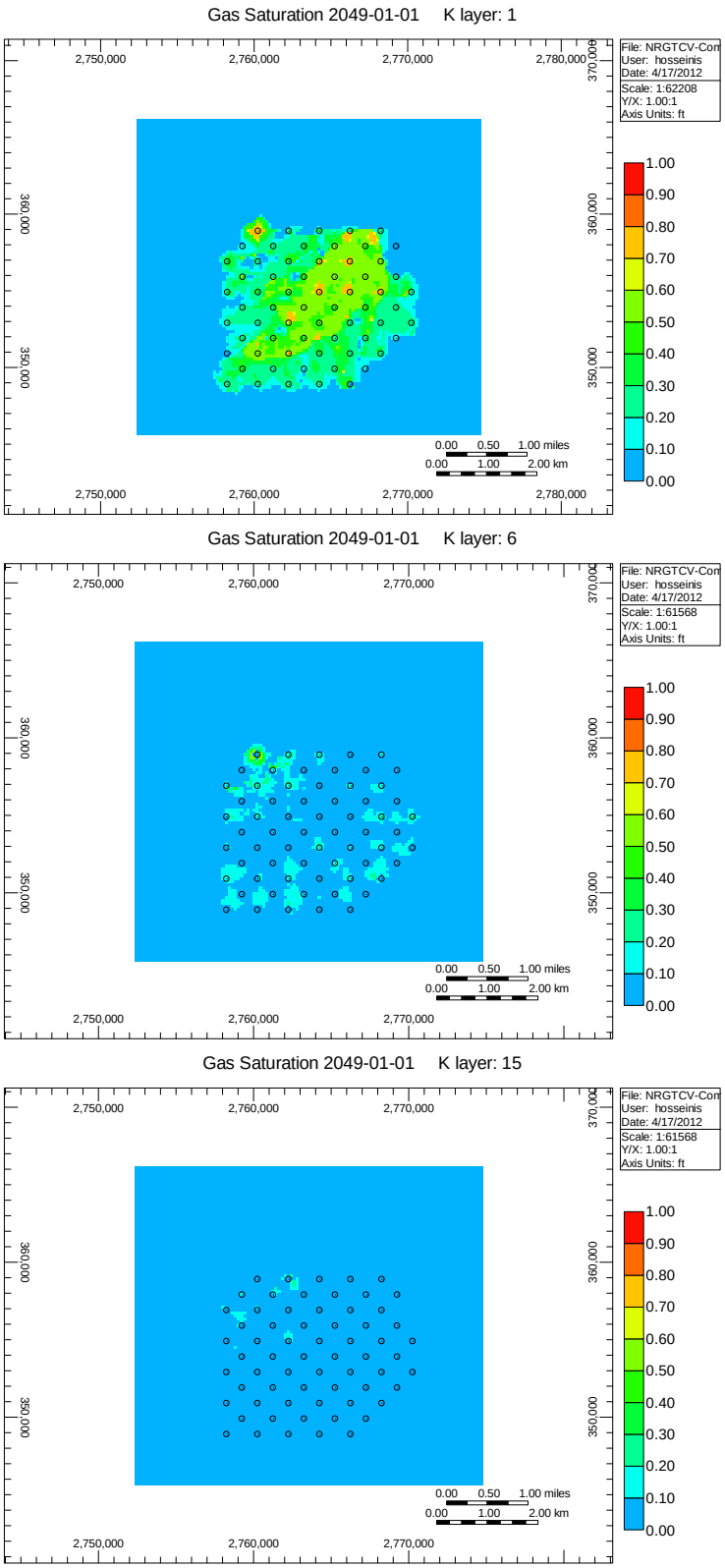

Fig 9. CO_2-A at 1/1/2049 in layers 1 (top), 6 and 15 (bottom), 30 years after termination of injection.

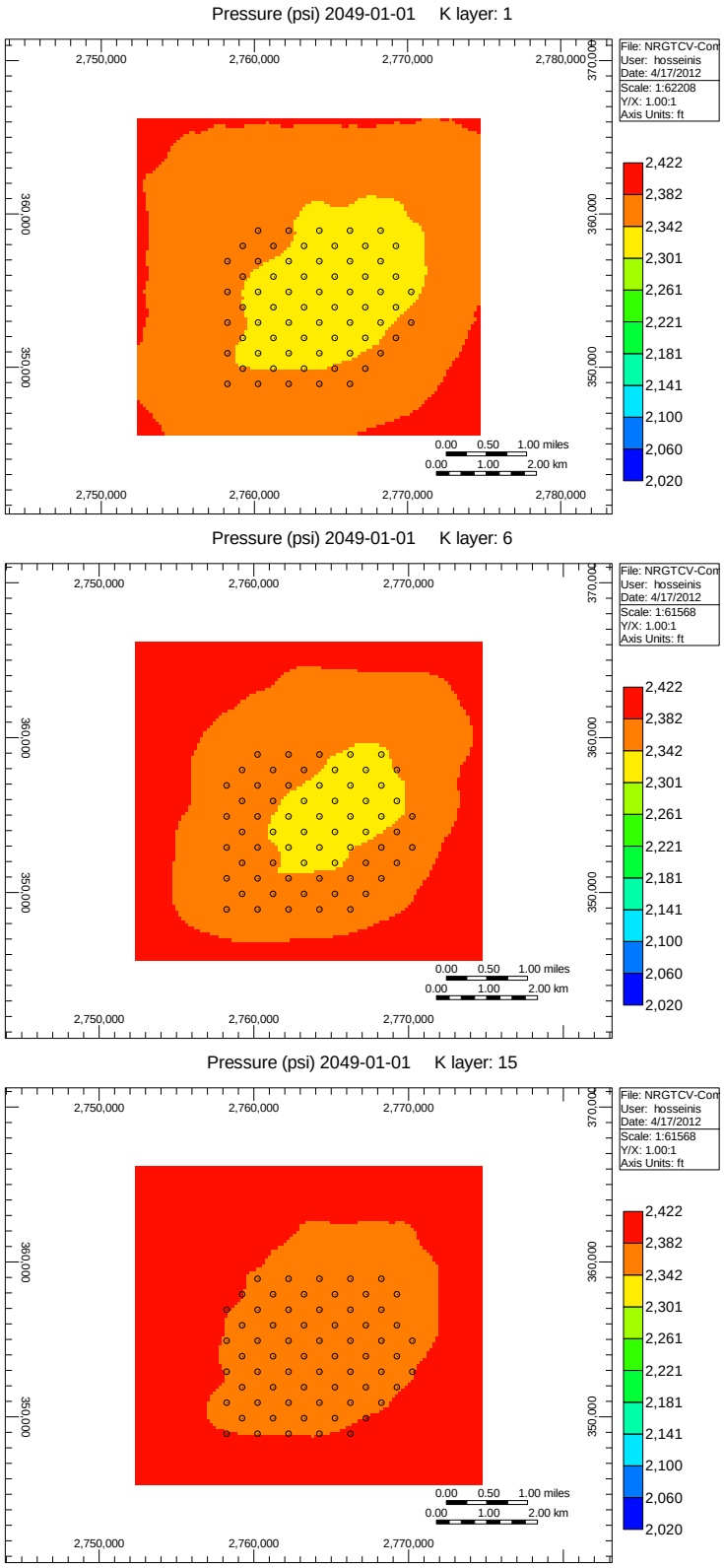

Fig 10. Pressure distribution at 1/1/2049 in layers 1 (top), 6 and 15 (bottom), 30 years after termination of injection.

Based on the assumed pattern of injection and production wells, and an injection rate of 1.7 million metric tonnes of CO_2, we show conformance of the operation. That is, both the injectate CO2-A and areas of elevated pressure remain within the TCV lease areas. Note that pressure elevation is mostly dominated by the production wells (around 2,000 psi), so there is no risk associated with excess pressurization of the field. By 2049, CO_2 moves to the top of the formation and as the reservoir pressure is below initial reservoir pressure at discovery (2800 psi), the strong regional aquifer will pressurize the reservoir back to about 2300 psi.

References

Galloway, W.E. and Cheng, E., 1985, Reservoir facies architecture in a microtidal barrier system – Frio Formation, Texas Gulf Coast, The University of Texas at Austin, Bureau of Economic Geology, Report of Investigations 144, 36p.

ICF Resources and Bureau of Economic Geology, 1989, As assessment of the reserve growth potential of the Frio Barrier-Strandplain play in Texas: contract report prepared for the U.S. Department of Energy/Office of Fossil Energy, 128p.

INTENTIONALLY LEFT BLANK

APPENDIX I

BEG FAULT STUDY REPORT

INTENTIONALLY LEFT BLANK

Evaluation of regional subsurface faulting in support of the West Ranch oilfield NEPA/EIS

Gulf Coast Carbon Center, Bureau of Economic Geology, Jackson School of Geosciences, The University of Texas at Austin

May 18, 2012

Summary

It is anticipated that anthropogenic carbon dioxide will be injected into the deep (~5,000-6,000 ft below sea level) subsurface for enhanced oil recovery (EOR) at the West Ranch oilfield in Jackson County, Texas beginning in early 2015. The purpose of this report is to present an evaluation of regional subsurface faulting in the vicinity of the oilfield to support National Environmental Policy Act, Environmental Impact Statement (NEPA/EIS) requirements for the NRG Energy Company's Clean Coal Power Initiative project being funded, in part, by the U.S. Department of Energy, National Energy Technology Laboratory (NETL). The primary geologic formation from which oil and gas are produced in the West Ranch field is the Frio Formation (Fm.). In Jackson County along the central Texas Gulf coast, the Frio Fm. was deposited in a marine beach setting (i.e. barrier-strand-plain) rather than a fluvial-deltaic setting as along northeast and southwest sections of the Texas Gulf Coast. In the northeastern areas, oil and gas were trapped primarily in salt domes. Unlike fields that produce from Frio Fm. salt domes, oilfields along the central Texas coast have little to no associated internal faulting.

The BEG geophysical-log-based evaluation of regional structural features shows two normal faults (growth faults) in the deep subsurface to the northwest and southeast of the West Ranch oilfield. The shallowest expression of the two faults is at depths of ~2,500 ft below sea level. An ~200 ft offset of geologic strata on either side of the fault to the northwest of the oilfield reveals the simple domal structure that is responsible for hydrocarbon trapping in the West Ranch field. Neither of the faults extend upward to land surface nor do they lie within the boundaries of the oilfield. In addition, there are no obvious or large-scale faults within the oilfield itself.

Introduction

The Frio Fm. is an Oligocene-age geologic unit that is present between ~5,000 and 6,500 ft below sea level in the West Ranch oilfield (fig. 1). Much of the Frio Fm. of the central Texas Gulf Coast was deposited as barrier-island/lagoonal systems (i.e., barrier-strand-plain) in ancient, near-shore beach environments (Boyd and Dyer, 1964; Galloway et al., 1982). According to Boyd and Dyer (1964), barrier strand-plain systems are composed of "elongate bodies of laterally deposited shoreline sands, similar to the Padre-Mustang-St. Joseph-Matagorda island complex of today." The depositional setting for Frio Fm. sediments along the northeastern and southwestern portions of the Texas Gulf coast was fluvial-deltaic (Galloway et al., 1982). In addition, deposits in the northeast are underlain by thick accumulations of Jurassic-age salt (Ewing, 1991). Thick accumulations of interlayered marine and nonmarine sand and shale of the Frio Fm. comprise one of the most prolific oil and gas producing geologic units in the Texas Gulf coast region (Galloway et al., 1982). Differences in depositional settings and subsequent geologic processes have resulted in different characteristics of Texas Gulf coast, Frio Fm. oilfields. For example to the northeast, hydrocarbons have been trapped in complexly

faulted salt dome structures whereas along the central Texas coast, simpler structural trapping has occurred (e.g. the West Ranch field).

Repeated pulses of rapidly deposited, large volumes of terrigenous sediment onto under-compacted, plastic muds in the Gulf of Mexico resulted in multiple stages of faulting along the northwestern margin throughout Tertiary time. Figure 2 shows the numerous growth faults that have been recognized in the western Gulf of Mexico basin. Growth faults, which are different from the type of faults that occur in salt domes, are a result of differential compaction and diagenesis of the different sediment packages. Bruce (1973) described the stages of growth faulting as:

- Interlayered sandstone and shale (terrigenous sediments) deposited on top of submarine shale masses
- Subsidence from sediment load accompanied by early water loss from underlying saturated shale masses
- Dewatering of shale masses becomes restricted and pore pressures increase
- Dewatering of sandstone/shale packages continues through the permeable sandstone layers
- Combination of greater compaction of sandstone/shale packages and increased pore pressure in shale masses (less compacted) results in uplift of shale masses relative to sandstone/shale
- Growth faulting results from instability and gravity sliding between the different sediment packages.

Figure 3 depicts results of the processes described above. The West Ranch oilfield is thought to lie within a sedimentary trough similar to that labeled #1 in figure 3 (HEC, personal communication).

Dr. Khandakar Zahid and Mr. David Carr, Postdoctoral Fellow and Research Scientist Associate, respectively with the Gulf Coast Carbon Center at the Bureau of Economic Geology, Jackson School of Geosciences, The University of Texas at Austin conducted geophysical log correlations, and construction of cross sections and maps to document the presence or absence of faulting in the vicinity of the West Ranch oilfield as described below.

Approach

The way to document the presence or absence of faulting is to correlate or match surfaces of geologic units laterally in the subsurface using geophysical logs. The top of the Anahuac shale, a geologic unit that immediately overlies the Frio Fm. (fig. 1), is a good horizon to use in such correlations because it is present throughout the subsurface of the Texas Gulf coast, has a distinctive geological log signature, and has several recognizable biostratigraphic zones (Ellisor, 1944). It is approximately 500 ft thick in the West Ranch field and pinches out within ~30 miles updip from the coast. Other strata used in this fault study are the individual reservoir sands within the Frio Fm. and the shallower Miocene interval (fig. 1).

Zahid and Carr evaluated the geological structure within and surrounding the West Ranch oilfield using a Petra© geological modeling project, which was assembled by Zahid and BEG graduate students using geophysical logs obtained from multiple commercial suppliers and augmented with those obtained from HEC. The presence of regional, down to the coast normal

faults (growth faults) close to West Ranch, and the absence of faulting within the oilfield have been previously documented in published literature (e.g., Baurenschmidt, 1944; Galloway and Cheng, 1986, Ewing, 1991, and Geomap, 1999-2009). These sources served as a starting point for the BEG results described below.

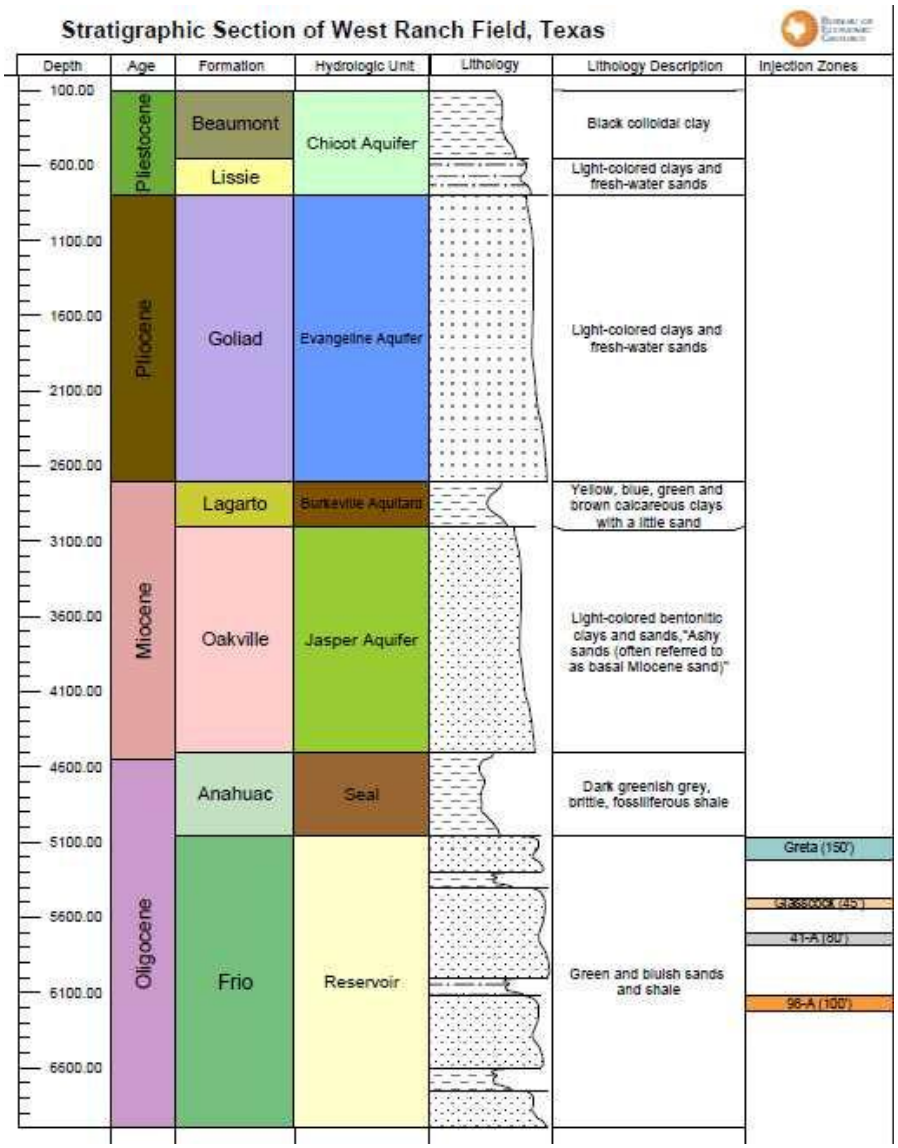

Figure 1. Geologic strata present at the West Ranch oilfield.

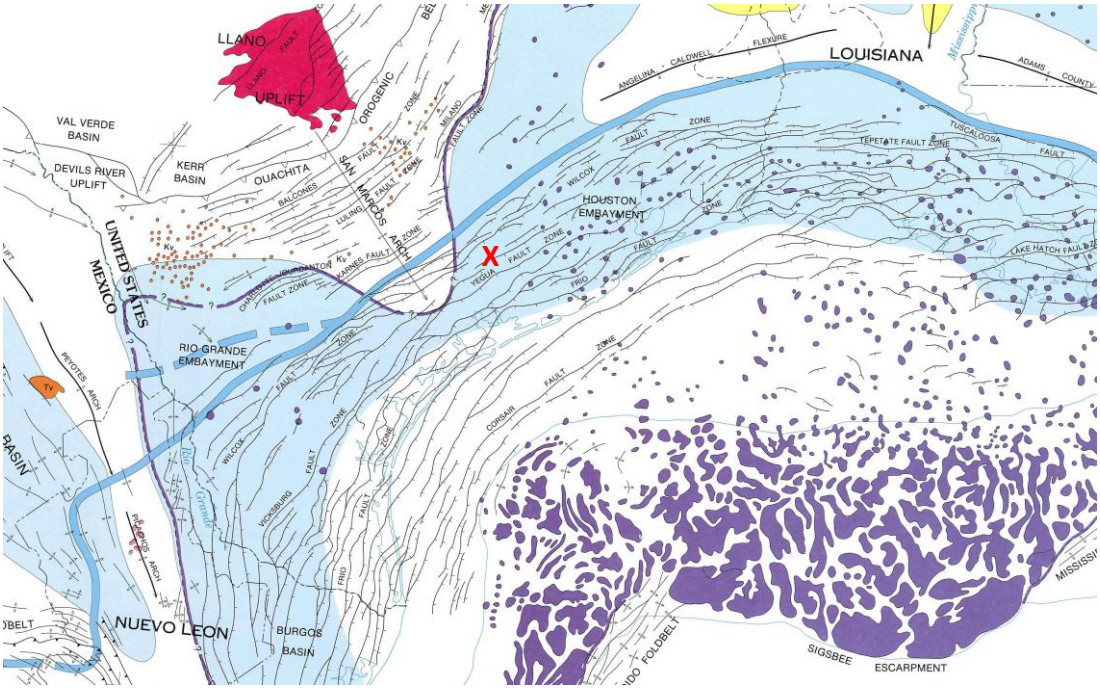

Figure 2. Structural features of the northwestern Gulf of Mexico basin. Modified from Ewing (1991), Plate 2. Red "X" shows approximate location of the West Ranch oilfield. Growth faults are thin black curved lines. Gulf coast outlined in light blue. Purple masses and dots (onshore and offshore) are salt structures (diapirs, pillows, or other structures).

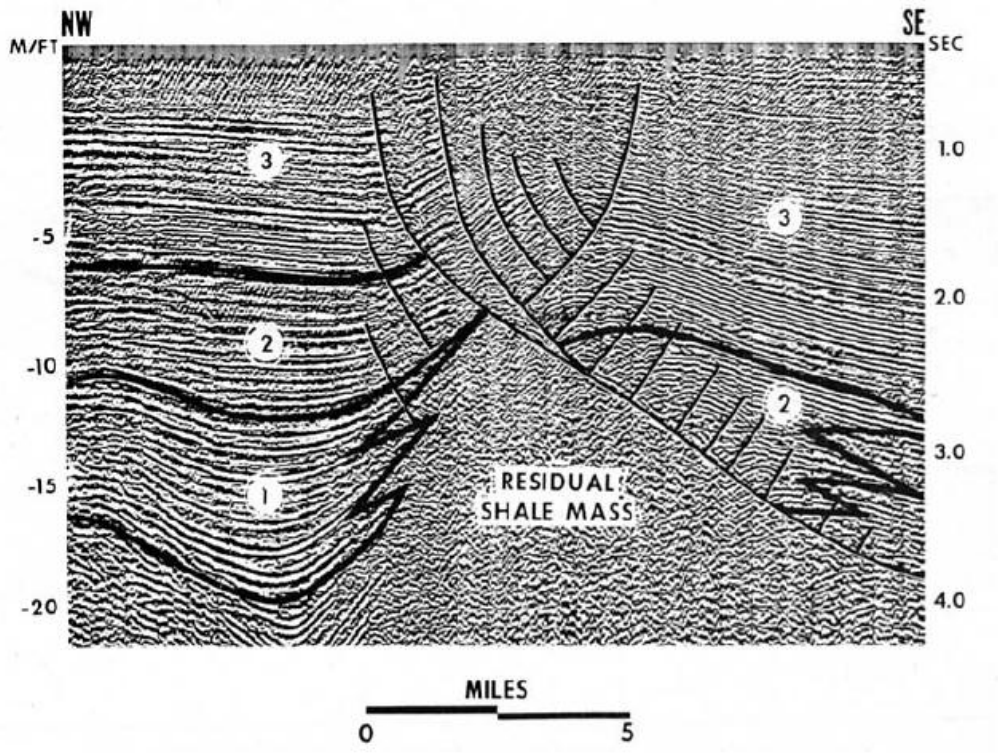

Figure 3. Seismic illustration of a submarine shale mass flanked by sandstone/shale sedimentary packages (1, 2, and 3) that have been offset by growth faulting (Bruce, 1973.

Results

As mentioned previously, published literature indicates that major growth faults are present near both the northwestern and the southeastern boundaries of the West Ranch oilfield. Figure 4 shows the West Ranch oilfield in Jackson County, Texas as defined by the concentration of geophysical logs; green dots represent oil wells. Locations of cross sections (blue lines) used to document vertical offset of the geologic strata on either side of the recognized faults (purple hatched lines) are also shown (fig. 4).

Both of the faults are mapped at the top of Anahuac shale (biostratigraphic zone *Discorbis*) in figure 4. Although the previously reported same two faults were mapped on different stratigraphic horizons [i.e., the GeoMap (1999-2009) faults were mapped at the top of Vicksburg Formation and the Galloway et al. (1986) fault was mapped on top of Miocene Formation], orientation of the faults are at high angle (80-85^{o}). As a result, both fault planes are at proximal distance to all reported stratigraphic intervals as seen in map view. The two faults set up the subtle roll-over anticlinal structure, which is located on the hanging wall immediately south of the down-to-the-basin fault to the northwest of the field (fig. 5). A roll-over anticline is a typical structure that has trapped hydrocarbons in many of the shallow Gulf coast oilfields (Ewing, 1991). As described by Nelson (1991), the subtle downward flexure or roll of beds on the downthrown (southeastward) side of the northwestern fault resulted from vertical collapse of the geological strata as the downthrown side moved away from the steeply dipping part of the fault. The more movement there is along such faults, the greater amount of roll of beds there will be on the downthrown side (Nelson, 1991). Given the very slight curvature or roll of surfaces marking the top of Anahuac and underlying reservoir sands (fig. 5), we can assume little movement along this fault.

Cross section A-A' is constructed of 13 logs hung on a sea level datum, is nine miles long, shows ~6,000 ft of geologic section, and runs perpendicular to the northwestern fault (fig. 5). Subsurface lithology and stratigraphy in each well can be interpreted from the log curves on the cross section, particularly the self potential (blue) and electrical resistivity (red) curves on each log. The fourth well from left in figure 4 does not contain digital log curves, only a raster image of the original well log. Raster images are just as useful in making this type of structural interpretation. The fault on cross section A-A' clearly offsets Anahuac shale and Greta sand horizons. We have extended it up into Miocene strata because of the offset observed in a small sand spike ~1,500 ft above the top of the Anahuac. The fault is dashed at depth because of the lack of geophysical log coverage. Figure 6 is another version of cross section A-A' plotted at true horizontal scale with an inset box showing the location of the zoomed-in view in fig. 7. In fig. 7, it is easier to see the vertical offset of ~150 ft in the Anahuac shale.

Cross section B-B' (fig. 8) is an 11-well, 4.5-mile long structural cross-section, shows ~7,000 ft of geologic section, and is perpendicular to the southeastern fault. It also shows the three target reservoir sands (Greta, 41-A and 98-A) and the overlying Anahuac shale. Most of the logs on the northwestern side of this fault only show section down through the Greta sand because we had not updated the Petra project with additional logs from Hilcorp at the time the cross sections were completed. The Anahuac is present on both sides of the fault showing a structural displacement of ~140 ft on the downthrown (northwestern) side of the fault.

Since early days of exploration and description the West Ranch field has been reported to be free of major faulting (e.g., Bauernschmidt, 1944). To complement the cross sections, a

structure-contour map of the Greta Sand (fig. 9) was made from analysis of logs from 600 wells in the main part of West Ranch field and its southwestward extension. Within the oilfield itself, the map clearly demonstrates the gentle four-way closure of the main anticline and a smaller closed structure to the southwest. Even with a tight contour interval of 10 feet, the contours are fairly smooth and regular, suggesting that no large-scale faulting, namely faults with throw exceeding 10-20 feet, exist in the field proper, where EOR activities will be focused.

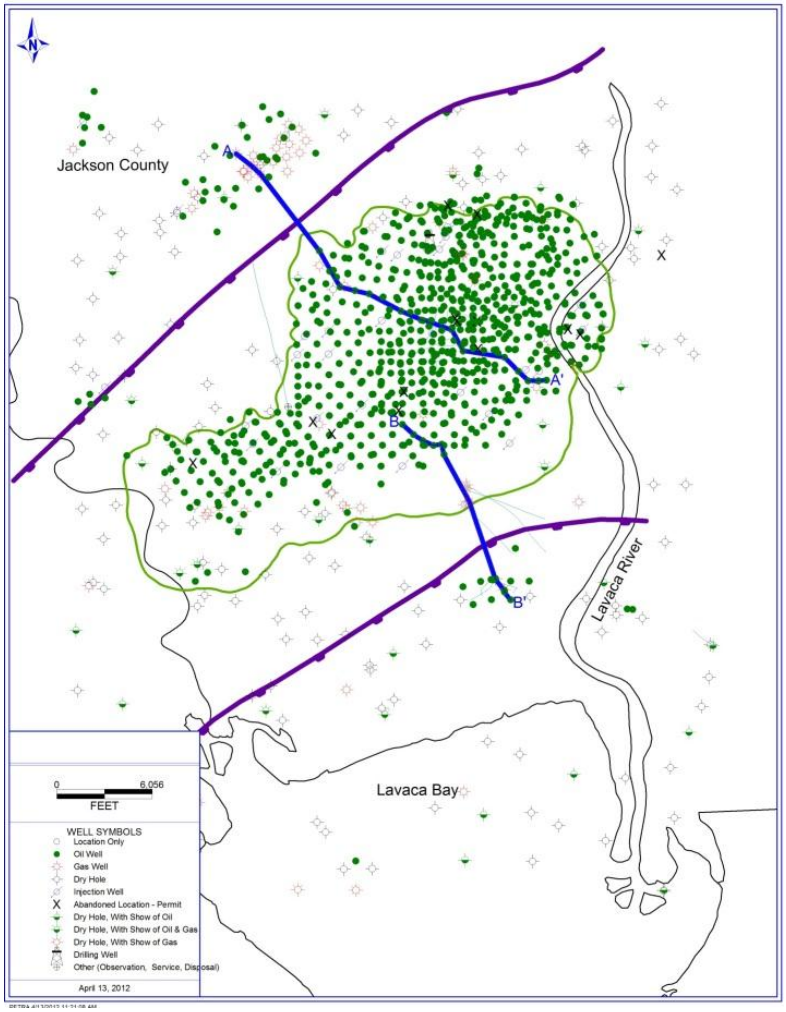

Figure 4. Map of West Ranch oilfield showing location of geophysical logs (see insert for key to well types), cross sections A-A' and B-B' (blue lines), and location of growth faults (purple lines) projected to the surface from the approximate top of the Anahuac Fm.

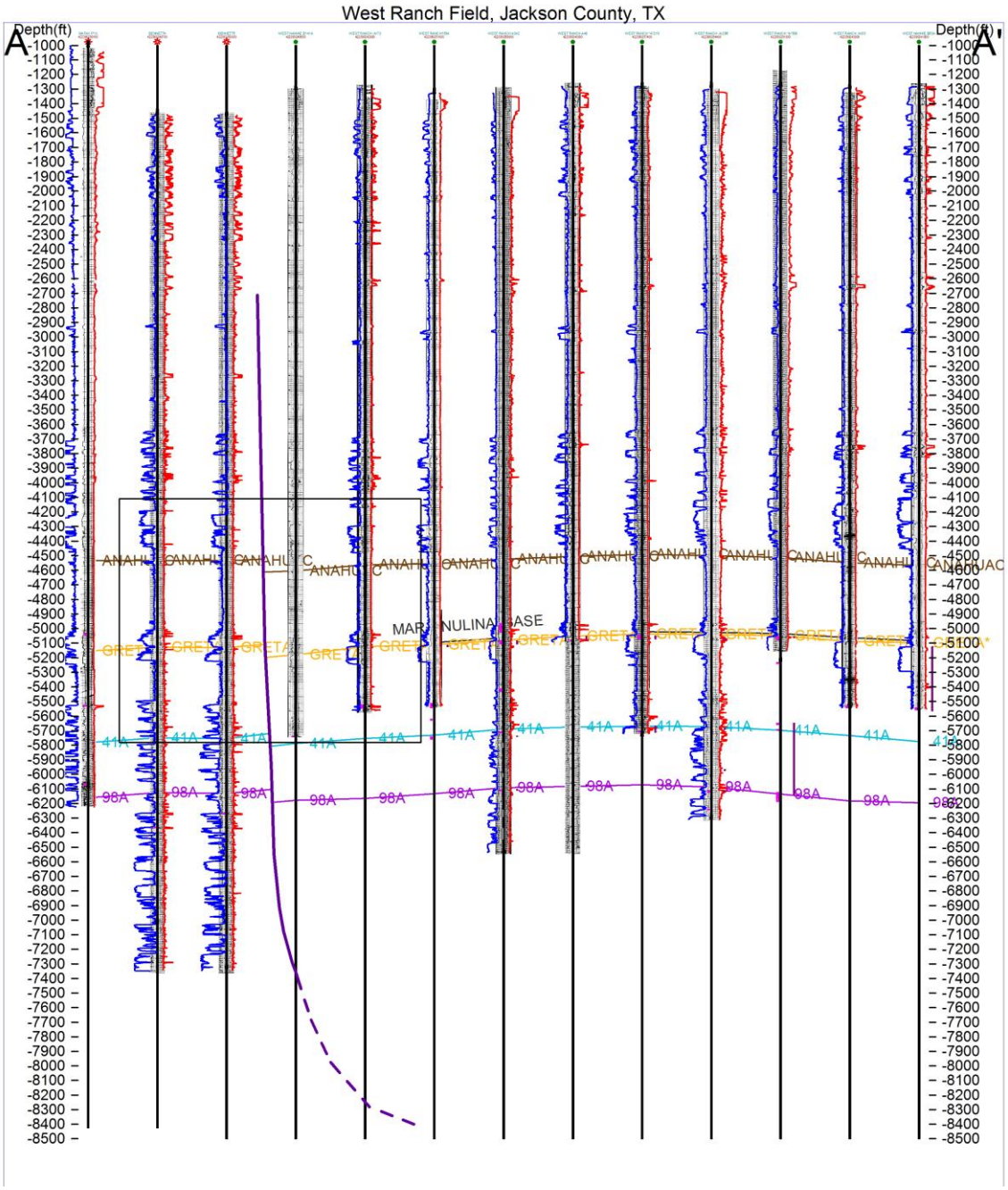

Figure 5. Cross section A-A'.

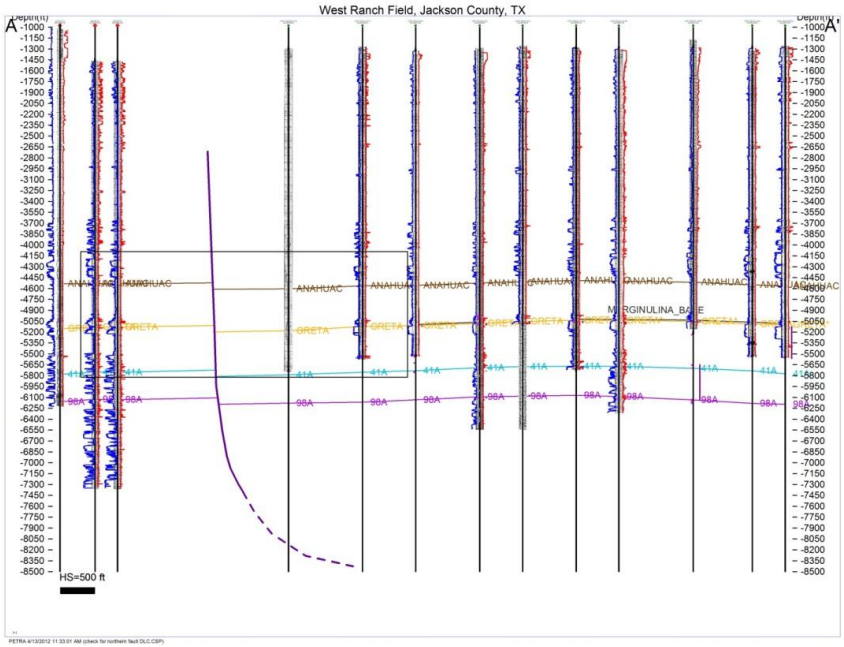

Figure 6. Version of cross section A-A' with true horizontal scale with box showing location of zoomed-in view in figure 7.

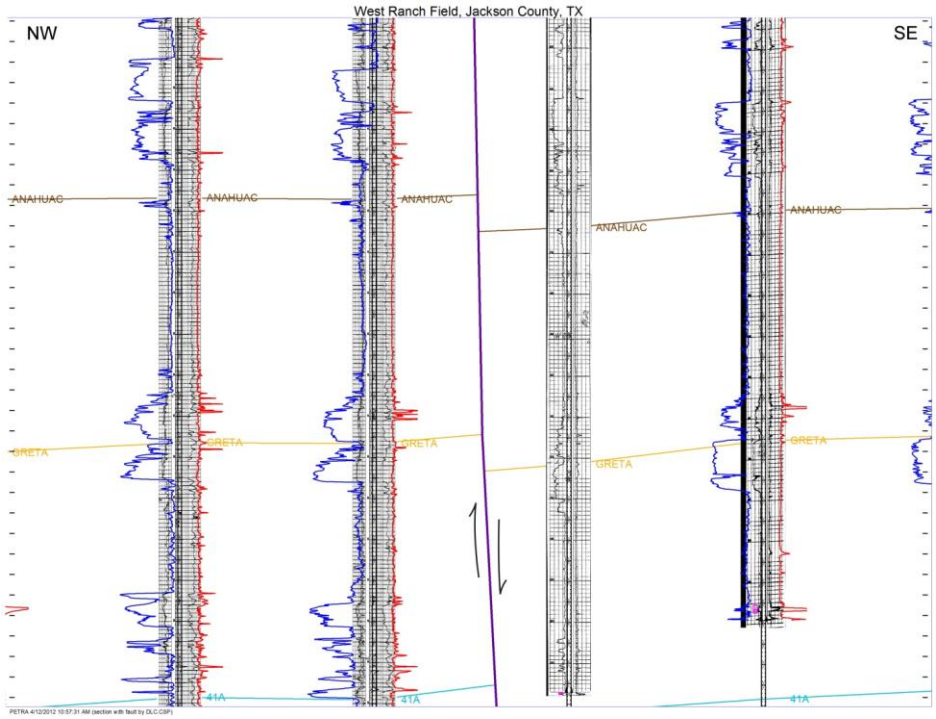

Figure 7. Zoomed-in view of box in cross section A-A'.

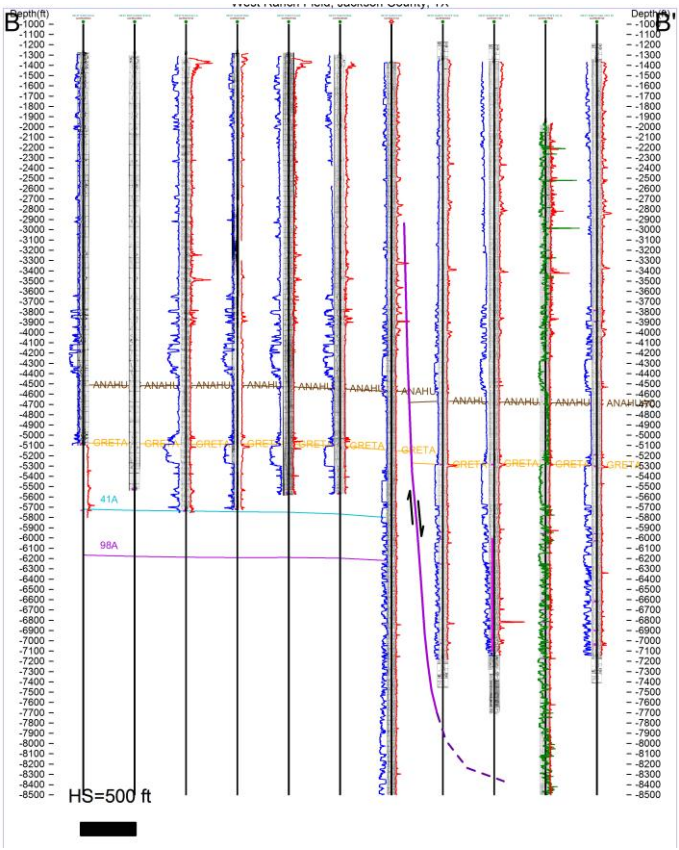

Figure 8. Cross section B-B’

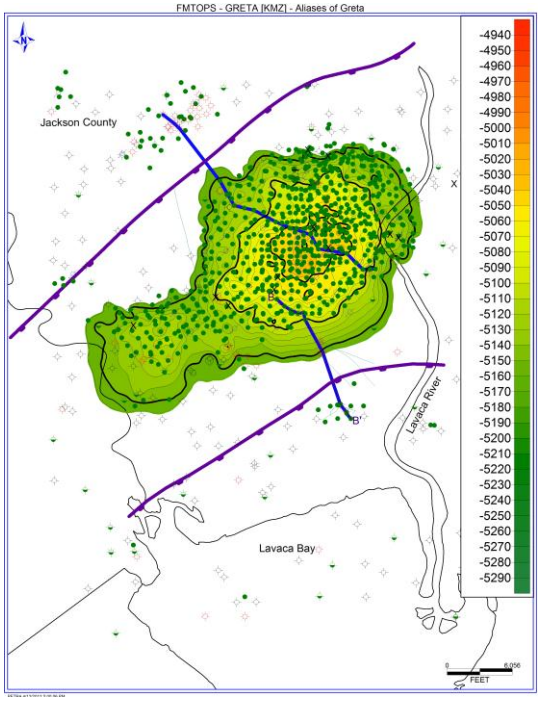

Figure 9. Structure contour map at the top of Greta sand using information for over 600 wells at West Ranch field. Contour interval = 10 feet.

References

Bauernschmidt, A. J., Jr., 1944, West Ranch oilfield, Jackson County, Texas: AAPG Bulletin v. 28, p. 197-216,

Bruce, C. E., 1973, Pressured shale and related sediment deformation: mechanism for development of regional contemporaneous faults, AAPG Bulletin, v. 57, p. 878-886.

Ellisor, A. C., 1944, Anahuac Formation, AAPG Bulletin, v. 28, p. 1355-1375.

Ewing, T. A., 1991, Structural framework, *in* Salvador, A., ed., 1991, The Gulf of Mexico Basin: Boulder, Colorado, Geological Society of America The Geology of North America, vol. J, 568 p.

Galloway, W. E., Hobday, D. K., and Magara, K., 1982, Frio Formation of the Texas Gulf Coast Basin – depositional systems, structural framework and hydrocarbon origin, migration, distribution and exploration potential: The University of Texas at Austin, Bureau of Economic Geology Report of Investigations 122, 36p.

Galloway, W. E. and Cheng, E., 1985, Reservoir facies architecture in a microtidal barrier system – Frio Formation, Texas Gulf Coast, The University of Texas at Austin, Bureau of Economic Geology, Report of Investigations 144, 36p.

GEOMAP Map Services, http://www.geomap.com/mapserv.html

Nelson, T. H., 1991, Salt tectonics and listric-normal faulting *in* Salvador, A., ed., 1991, The Gulf of Mexico Basin: Boulder, Colorado, Geological Society of America The Geology of North America, vol. J, 568 p.